Neuro-Oncology Advances

1(1), 1–15, 2019 | doi:10.1093/noajnl/vdz011 | Advance Access date 28 August 2019

Integrated models incorporating radiologic and radiomic features predict meningioma grade, local failure, and overall survival

Olivier Morin[†], William C. Chen[†], Farshad Nassiri, Matthew Susko, Stephen T. Magill, Harish N. Vasudevan, Ashley Wu, Martin Vallières, Efstathios D. Gennatas, Gilmer Valdes, Melike Pekmezci, Paula Alcaide-Leon, Abrar Choudhury, Yannet Interian, Siavash Mortezavi, Kerem Turgutlu, Nancy Ann Oberheim Bush, Timothy D. Solberg, Steve E. Braunstein, Penny K. Sneed, Arie Perry, Gelareh Zadeh, Michael W. McDermott, Javier E. Villanueva-Meyer[‡], and David R. Raleigh[‡]

Department of Radiation Oncology, University of California San Francisco, California (O.M., W.C.C., M.S., H.N.V., A.W., M.V., E.D.G., G.V., A.C., Y.I., S.M., K.T., T.D.S., S.E.B., P.K.S., D.R.R.); Department of Surgery, University of Toronto, Toronto, Ontario, Canada (F.N., G.Z.); Department of Neurological Surgery, University of California San Francisco, California (S.T.M., A.C., N.A.O.B., A.P., M.W.M., D.R.R.); Department of Pathology, University of California San Francisco, California (M.P., A.P.); Department of Radiology and Biomedical Imaging, University of California San Francisco, California (P.A.L., J.E.V-M.)

Corresponding author: David R. Raleigh, MD, PhD, Departments of Radiation Oncology and Neurological Surgery, University of California San Francisco, 505 Parnassus Avenue, L08/L75, Box 0226, San Francisco, CA 94143, USA (david.raleigh@ucsf.edu)
[†]These authors contributed equally to this work.
[‡]These authors contributed equally to this work.

Abstract

Background. We investigated prognostic models based on clinical, radiologic, and radiomic feature to preoperatively identify meningiomas at risk for poor outcomes.

Methods. Retrospective review was performed for 303 patients who underwent resection of 314 meningiomas (57% World Health Organization grade I, 35% grade II, and 8% grade III) at two independent institutions, which comprised primary and external datasets. For each patient in the primary dataset, 16 radiologic and 172 radiomic features were extracted from preoperative magnetic resonance images, and prognostic features for grade, local failure (LF) or overall survival (OS) were identified using the Kaplan–Meier method, log-rank tests and recursive partitioning analysis. Regressions and random forests were used to generate and test prognostic models, which were validated using the external dataset.

Results. Multivariate analysis revealed that apparent diffusion coefficient hypointensity (HR 5.56, 95% CI 2.01–16.7, $P = .002$) was associated with high grade meningioma, and low sphericity was associated both with increased LF (HR 2.0, 95% CI 1.1–3.5, $P = .02$) and worse OS (HR 2.94, 95% CI 1.47–5.56, $P = .002$). Both radiologic and radiomic predictors of adverse meningioma outcomes were significantly associated with molecular markers of aggressive meningioma biology, such as somatic mutation burden, DNA methylation status, and *FOXM1* expression. Integrated prognostic models combining clinical, radiologic, and radiomic features demonstrated improved accuracy for meningioma grade, LF, and OS (area under the curve 0.78, 0.75, and 0.78, respectively) compared to models based on clinical features alone.

Conclusions. Preoperative radiologic and radiomic features such as apparent diffusion coefficient and sphericity can predict tumor grade, LF, and OS in patients with meningioma.

Key Points

1. Models incorporating imaging information provide improved estimates of meningioma outcomes.
2. ADC and sphericity are prognostic imaging-derived factors for meningioma.

Importance of the Study

Meningioma is the most common primary intracranial tumor in the United States. Outcomes from meningioma are influenced by patient age, sex, tumor grade, extent of resection, and adjuvant radiotherapy. Here, we perform a comprehensive qualitative and quantitative imaging analysis to integrate traditional prognostic variables with preoperative radiologic and radiomic features to develop integrated models for meningioma outcomes. We find that models incorporating radiologic and radiomic data with demographic and clinical information provide the best accuracy for predicting meningioma outcomes preoperatively. Moreover, we identify apparent diffusion coefficient and sphericity as prognostic imaging-derived features that can be used to identify meningioma patients at risk for poor clinical outcomes.

Meningiomas, which display remarkable histopathologic and clinical heterogeneity, represent approximately 37% of all primary intracranial tumors diagnosed in the United States.[1,2] Although clinical features such as adjuvant radiation, patient age, and history of prior meningioma influence outcomes for patients with meningioma, the primary prognostic features are World Health Organization (WHO) grade and extent of resection.[3] The majority of meningiomas are WHO grade I and follow an indolent clinical course, particularly after gross total resection (GTR) or definitive radiotherapy.[4] However, some WHO grade I and a substantial proportion of WHO grade II (atypical), and WHO grade III (anaplastic) meningiomas have high rates of local failure (LF) ranging from 20% to 70% at 5 years despite multimodal treatment with surgical resection and adjuvant radiotherapy.[5–8] Thus, meningioma grade and extent of resection are useful markers for risk stratification, but do not fully capture the diversity of meningioma biology or clinical behavior. Consequently, there is an unmet clinical need for new prognostic markers to identify meningiomas at risk for poor clinical outcomes.

Imaging is acquired for all meningioma patients prior to surgery or radiation, and represents a potential source of useful prognostic information. In that regard, qualitative investigations of meningioma magnetic resonance (MR) imaging have identified mushroom shape, peritumoral edema, bone involvement, proximity to a dural sinus, and greater tumor size, among others, as prognostic radiologic features of poor clinical outcomes.[9,10] Complementary to radiologic analyses, radiomics aims to identify morphologic, textural, and statistical imaging features that predict tumor biology and clinical behavior. Radiomic analyses have identified features with prognostic value for diverse human cancers,[11–17] and for meningioma, radiologic and radiomic features can be used to predict tumor grade, but the utility of these techniques to prognosticate clinical outcomes is unknown.[12] Thus, to preoperatively identify meningiomas at risk for poor outcomes, we performed a comprehensive MR imaging analysis of 303 meningiomas (57% WHO grade I, 35% grade II, and 8% grade III) resected at two independent institutions to discover the most important radiologic and radiomics features associated with tumor grade, LF, and overall survival (OS). Using these findings, we developed integrated prognostic models to guide future strategies for meningioma risk stratification (Supplementary Figure 1), and identify apparent diffusion coefficient (ADC) and sphericity as prognostic imaging-derived features that can be used to preoperatively identify meningioma patients at risk for poor clinical outcomes.

Methods and Materials

Inclusion Criteria and the Primary Dataset

Patients with (1) comprehensive clinical and demographic data, (2) preoperative imaging suitable for qualitative and quantitative analyses, and (3) sufficient tissue for pathologic evaluation who underwent resection of meningioma were eligible. Patients meeting these criteria at the University of California San Francisco (primary dataset) from 1990 to 2017 were retrospectively identified and included in this study. Approximately 2600 patients underwent resection of meningioma at the University of California San Francisco during that period, and of the 218 patients who met inclusion criteria, all cases diagnosed prior to 2007 were re-evaluated by board certified neuropathologists using contemporary diagnostic criteria.[1] This study, and our preceding molecular analysis of meningiomas,[18] were both approved by the Institutional Review Board, Human Research Protection Program Committee on Human Research, at the University of California San Francisco, and written informed consent for participate in research was obtained from patients at the time of surgery.

Patient demographic, past medical history, and treatment variables were extracted from the medical record. These included patient age at the time of resection, sex, race, history of prior head or neck radiotherapy, history of prior meningioma treatment, extent of resection, and adjuvant radiotherapy (Table 1). GTR (Simpson grade I-III) and subtotal resection (Simpson grade IV) were determined based on postoperative imaging in conjunction with the operative report. LF was determined radiologically and defined as the appearance of any tumor locally on subsequent brain imaging following GTR or interval growth of residual tumor of ≥20% along any dimension following subtotal resection. Local freedom from recurrence (LFFR) and OS were determined from the date of meningioma resection until the date of LF or death, respectively. The date of last contact was used for survival analysis for patients who were alive and without

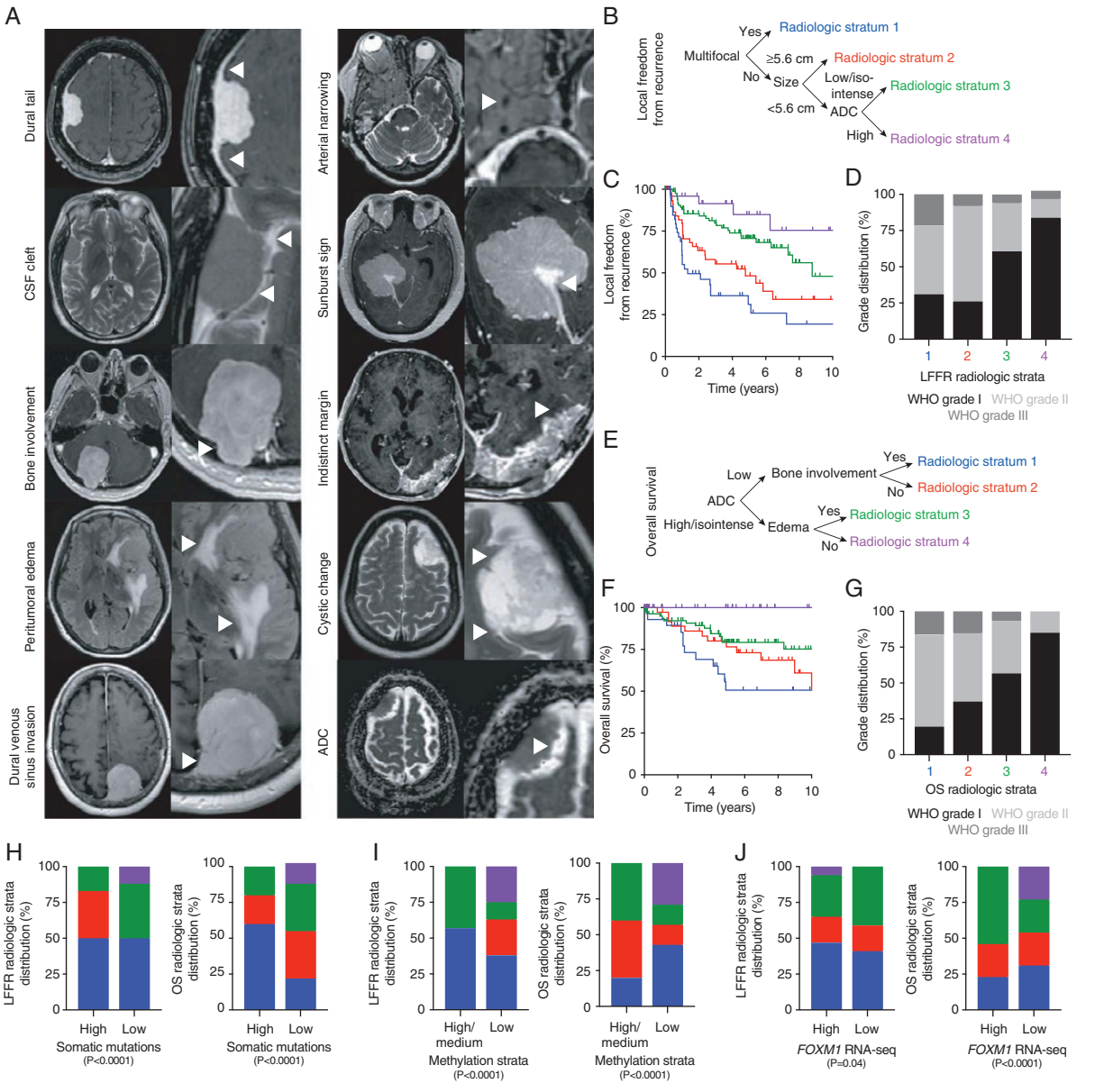

Fig. 1 Radiologic features with prognostic significance for meningioma. (**A**) Examples of radiologic features annotated on preoperative MR images, such as axial T1 post-contrast image showing a dural tail (arrows) from a right frontal meningioma, axial T2 image showing a CSF cleft sign (arrows) from a right temporal meningioma, axial T1 post-contrast image showing bony involvement (arrow) of the right occipital bone from a right cerebellar meningioma, axial FLAIR image showing peritumoral edema (arrows) from a left frontal meningioma, axial T1 post-contrast image showing dural venous sinus invasion (arrow) from a left posterior parasagittal meningioma, axial T2 image showing narrowing of the right internal carotid artery flow void (arrow) from a multi-compartmental right skull base meningioma, axial T1 post-contrast image showing a "sunburst" sign (arrow) in a right tentorial meningioma, axial T1 post-contrast image showing an indistinct tumor margin with brain parenchyma (arrow) from a left occipital meningioma, axial T2 image showing cystic changes (arrows) in a left frontal meningioma, and an ADC map showing signal hypointensity (arrow) in a right frontal meningioma. (**B**) RPA identifies four distinct LF risk strata for meningioma based on radiologic features of multifocality, maximal tumor diameter, and ADC intensity. (**C**) Kaplan–Meier curves for radiologic meningioma LF risk strata identified by RPA ($P < .0001$, log-rank test). (**D**) Grade distribution within radiologic meningioma LF risk strata ($P < 0.0001$, chi-square test). (**E**) RPA identifies three distinct risk strata for OS from meningioma based on radiologic features of ADC intensity, peritumoral edema, and bone involvement. (**F**) Kaplan–Meier curves for radiologic meningioma OS risk strata identified by RPA ($P < .0001$, log-rank test). (**G**) Grade distribution within radiologic meningioma OS risk strata ($P < 10^{-6}$, chi-square test). (**H–J**) Meningiomas from high-risk radiologic strata have high somatic mutation burdens as identified by whole exome sequencing, high DNA methylation profiles, and high *FOXM1* expression as identified by RNA-seq, consistent with aggressive tumor biology.[18] Analyses are based on the primary dataset. The number of somatic mutations were dichotomized at the mean to assign mutation burden, methylation clusters were generated by unsupervised hierarchical clustering of the top 2000 most variable probes, and *FOXM1* expression from RNA-seq was dichotomized at the median.ADC, apparent diffusion coefficient; CSF, cerebrospinal fluid; FLAIR, fluid attenuated inversion recovery; LF, local failure; LFFR, local freedom from recurrence; MR, magnetic resonance; OS, overall survival; RNA-seq, RNA sequencing; RPA, recursive partitioning analysis; WHO, World Health Organization.

Table 1. University of California San Francisco (primary dataset) patients, meningiomas, imaging, treatments, and outcomes

Patients	218
Median age (range)	58.6 years (13.7–88.6 years)
Male:female (ratio)	81:137 (1:1.7)
Race	
Caucasian	152 (70%)
Hispanic	26 (12%)
Asian	21 (10%)
Black	10 (5%)
Other (not Hispanic/Latino)	9 (4%)
History of head or neck radiotherapy	10 (5%)
Multifocal meningioma	57 (26%)
Meningiomas	229
World Health Organization grade (2007)	
I	112 (49%)
II (atypical)	93 (41%)
III (anaplastic)	24 (10%)
Primary:recurrent (ratio)	189:68 (2.8:1)
Median size (range)	33.4 cm^3 (0.3–335.3 cm^3)
Imaging details	
Scanner GE:Phillips	222:7
Gradient echo sequence	All
Scans type T1 3D SPGR	All
1.5T:3T	163:66
Median slice thickness (range)	1.5 mm (1.2–3.0 mm)
Contrast gadolinium	All
Median repetition time (range)	34 ms (4.3–35 ms)
Median echo time (range)	3.2 ms (1.3–8.0 ms)
Radiologic findings	
Focality (solitary:multifocal)	180:39
Median largest diameter, size 1D (range)	4.4 cm (1.2–9.2 cm)
T1 (hypointense:isointense:hyperintense)	92:120:1
T1plus (degree of CE, none:mild:marked)	0:38:181
T2 (hypointense:isointense:hyperintense)	52:75:92
ADC (hypointense:isointense:hyperintense)	39:85:67
Peritumoral edema	164 (72%)
Necrosis or cystic change	26 (11%)
Indistinct margins	19 (8%)
Bone involvement	86 (38%)
Venous sinus involvement	44 (19%)
Arterial narrowing	22 (10%)
CSF cleft	167 (73%)
Dura tail	213 (93%)
Sunburst	37 (16%)
Location	
Skull base	99 (38%)
Anterior cranial fossa	48 (21%)
Middle cranial fossa	51 (22%)
Posterior cranial fossa	32 (14%)
Convexity	139 (61%)

Table 1. Continued

Midline	106 (46%)
Treatment	
Extent of resection	
Gross total resection	128 (56%)
Subtotal resection	100 (44%)
Extent of resection unknown	1 (0.4%)
Adjuvant radiotherapy	55 (24%)
Outcomes	
Median follow-up (range)	52 months (0–197 months)
Local failure	92 (36%)
Median time to local failure (range)	16.2 months (1.7–196 months)
Death	60 (27%)
Median time to death (range)	42 months (0.8–173 months)
Cause of death	Progressive disease 28 (47%) Treatment 10 (17%) Other/unknown 22 (36%)

radiologic evidence of recurrence at last follow-up. Survival status of patients was determined by a combined search of electronic medical records; institutional cancer registry; the Surveillance, Epidemiology and End Results Program; the Department of Motor Vehicles; social security and nationwide hospital obituary databases; and publicly available obituaries.

External Dataset

An independent, external validation dataset consisting of patients who underwent resection of meningioma at the University of Toronto (external dataset) from 2010 to 2017 was developed using similar criteria. In brief, demographic, past medical history, and treatment variables were extracted from the medical record for 85 patients with preoperative imaging suitable for qualitative and quantitative analysis (Table 2). These data included patient age at the time of resection, sex, history of prior head or neck radiotherapy, history of prior meningioma treatment, extent of resection, adjuvant radiotherapy, meningioma grade, LF, and vital status, similar to the variables comprising the primary dataset. Consistently, this study was also approved by the Institutional Review Board, Human Research Protection Program Committee on Human Research, at the University of Toronto. Of note, there were fewer atypical and anaplastic meningiomas in the external dataset compared to the primary dataset (21% vs 51%), which corresponded to a decrease in the number of local recurrences (7% vs 36%) and deaths (6% vs 27%). Moreover, the median imaging follow-up in the external dataset was shorter than the primary dataset (40 months vs 52 months). Despite these limitations, the prognostic value of preoperative imaging features was recapitulated in the external dataset, and combination of primary and external datasets improved the performance of integrated prognostic models predicting tumor grade, LF, and OS in patients with meningioma.

MR Image Acquisition

Preoperative imaging for both the datasets was acquired exclusively on GE 1.5 or 3 Tesla MR scanners. The MR imaging parameters varied slightly over the course of the study period, but at a minimum, the standard neuronavigation MR imaging protocol consisted of the following pulse sequences: pre-contrast T1 and T2, T2 fluid attenuated inversion recovery (FLAIR), diffusion weighted (b values, 0 and 1000 s/mm^2), and gadolinium-enhanced 3D spoiled gradient-recalled echo (SPGR) T1-weighted images.

Annotation of Radiologic Features

A comprehensive radiologic review of preoperative imaging studies from both datasets was performed by board certified (J.E.V-M.) and fellowship trained (P.A-L.) neuroradiologists, who were blinded to all clinical data. Interrater reliability of radiologic annotations was measured using kappa statistics.[19] Commonly annotated radiologic characteristics were derived from multiplanar MR images, including maximal tumor diameter, intrinsic T1 signal intensity, degree of contrast enhancement on gadolinium-enhanced T1 imaging, T2 signal intensity, intratumoral necrosis, venous sinus involvement, presence of multiple meningiomas (multifocal), arterial narrowing, bone involvement, indistinct tumor margins, peritumoral edema, sunburst vessels, dural tail, cerebrospinal fluid (CSF) cleft sign, and meningioma location (Table 3). Location was classified with the following non-mutually exclusive categories: anterior cranial fossa,

Table 2. University of Toronto (external dataset) patients, meningiomas, imaging, treatments, and outcomes.

Patients	85
Median age (range)	59.0 years (18–89 years)
Male:female (ratio)	31:54 (1:1.7)
Prior radiation	7 (8.2%)
Multifocal meningioma	10 (11.8%)
Meningiomas	85
World Health Organization grade (2007)	
I	67 (78.8%)
II (atypical)	17 (20.0%)
III (anaplastic)	1 (1.2%)
Primary:recurrent	83:2
Median size (range)	23.6 cm^3 (0.5–236.4 cm^3)
Imaging details	
Scanner GE	All
1.5T:3T	81:4
Scans type T1 3D SPGR	All
Radiologic findings	
Median largest diameter, size 1D (range)	5.15 cm (1.3–13.5 cm)
ADC (hypointense:isointense:hyperintense)	19:35:18
Peritumoral edema	51 (60%)
Indistinct margins	13 (15.3%)
Bone involvement	21 (24.7%)
Treatment	
Extent of resection	
Gross total resection	48 (56.4%)
Subtotal resection	10 (11.8%)
Extent of resection unknown	27 (31.8%)
Adjuvant radiotherapy	4 (4.7%)
Outcomes	
Median follow-up (range)	39.5 months (0.13–174.15)
Local failure	6 (6.9%)
Median time to local failure (range)	20.6 months (6.5–56.7)
Death	5 (5.7%)
Median time to death (range)	11.5 months (0.13–28.4)
Cause of death	Other/unknown 5 (100%)

ADC, apparent diffusion coefficient.

middle cranial fossa, posterior cranial fossa, midline, convexity and/or skull base. In keeping with the clinical nature of radiologic annotations, ADC was evaluated qualitatively as would be in routine practice. Tumor signal intensity on ADC maps was recorded for patients for whom diffusion weighted imaging was available (N = 263, 84% of total). All signal intensities were measured relative to gray matter. Interrater reliability measured with kappa statistics for radiological features with prognostic significance was substantial, with k = 0.76 for ADC hypointensity, k = 0.7 for bone involvement, k = 0.85 for peritumoral edema and k = 0.63 for indistinct tumor margins.

Calculation and Selection of Radiomic Features

All meningiomas were manually segmented on preoperative three-dimensional T1 post-contrast MR images using commercially available software (MIM Software Inc.) by two radiation oncologists (W.C.C. and M.S.), and verified by a board-certified radiation oncologist with expertise in central nervous system tumors (D.R.R.). Images and contours were processed using a quantitative imaging prediction modeling platform named *MEDomicsLab*, which extracts radiomic features from MR images as described in the Imaging Biomarker Standardization Initiative.[20] Prior to feature calculation, MR images were bias corrected[21] in

Table 3. Prognostic model feature composition

Model	Features	Descriptions[a]
Demographic	Age	Continuous
	Sex	Male or female
	Race	White, black, Asian, Hispanic, Pacific Islander, American Indian, other
	Prior radiotherapy (RT)	Prior cranial radiotherapy
	Recurrent	Recurrent at presentation
Radiologic	Multifocal	
	Size 1D	Continuous
	T1	Hypointense, Isointense, and hyperintense[b]
	T1plus	Degree of contrast enhancement; none, mild
	T2	Hypointense, Isointense, and hyperintense
	ADC	Hypointense, Isointense, and hyperintense
	Peritumoral edema	
	Necrosis or cystic change	
	Brain invasion	
	Bone invasion	
	Venous	
	Arterial	
	CSF cleft	
	Dura tail	
	Sunburst	
	Skull base	
	Anterior cranial fossa	
	Middle cranial fossa	
	Posterior cranial fossa	
	Convexity	
	Midline	
Radiomics	Morphological (29)	Volume, shape, elongation, compactness, sphericity
	Filter: wavelet (8)	Coiflet filter applied
	Local intensity (1)	Local intensities within the segmented volume
	Statistical (18)	Mean, standard deviation, minimum, maximum, busyness, etc.
	Intensity Histogram (23)	Bin the intensities of the segmented volume
	Intensity Volume Histogram (7)	Bin the volume as it relates to intensities
	Texture: GLCM (25)	Occurrence of neighboring pixels
	Texture: GLSZM (16)	Volume sizes for given intensities
	Texture: GLDZM (16)	Distance between volumes of varying intensities
	Texture: NGTDM (5)	Distance between adjacent gray tone regions
	Texture: NGGLDM (17)	Distance between adjacent gray-level regions
Therapy	Extent of resection	Subtotal resection, gross total resection
	Adjuvant radiotherapy	
Grade	Grade	Grade I (low), and grade II and III (high)

ADC, apparent diffusion coefficient; CSF, cerebrospinal fluid; GLCM, gray-level co-occurrence matrix; GLRL, gray-level run length matrix; GLSZM, gray-level size-zone matrix; GLDZM, gray-level distance-zone matrix; NGTDM, neighborhood gray-tone difference matrix; NGGLDM, neighborhood gray-level dependence matrix.

[a]Unless otherwise stated, all variables were binary.

[b]Signal intensity measured relative to gray matter.

MIM and normalized using a segmented region of normal cortex to limit variability in signal intensity between patients. Likewise, expansions and contractions of segmented tumors ranging from 1 to 3 mm were generated to eliminate potential biases from small contouring variations prior to feature selection. The calculated radiomic features included 29 morphologic, 1 local intensity, 18 statistics, 23 intensity histogram, 7 intensity volume histogram, 25 gray-level co-occurrence matrix, 16 gray-level run-length matrix, 16 gray-level size-zone matrix (SZM), 16 gray-level distance-zone matrix (DZM), 5 neighborhood gray-tone difference matrix, and 16 neighborhood gray-level difference matrix (Table 3). Wavelet filters (coiflet base function) were also applied in three-dimensions prior to feature calculation. In addition to the original image space, radiomic features were also extracted from the resulting eight wavelet sub-bands. Feature extraction was performed using a scale of 3 mm and a quantization level of 32 fixed bins. For incorporation into prognostic models, the initially large set of radiomic features was reduced to fewer than 15 features using a supervised false-positive avoidance methodology[22] to reduce feature correlation and dimensionality. The reduced set of radiomic features was retained for all random forest models thereafter (Table 3).

Statistical Analyses

Five sets of features were used to develop prognostic models: (1) demographic features at presentation, (2) radiologic features annotated from preoperative MR imaging, (3) radiomic features extracted from preoperative three-dimensional T1 post-contrast MR images, (4) therapeutic characteristics such as extent of resection and adjuvant radiation, and (5) meningioma grade as established by histopathologic analysis (Supplementary Figure 1 and Table 3). All random forest models were trained and tested using nested resampling. For each model, 1000 random forest trees were generated. The primary and external datasets were split into three sets each time, including a training set (70%), a validation set (10%), and a testing set (20%). The training and validation sets derived from the primary dataset were used for hyperparameter tuning using grid search and final feature selection. Once the optimal hyperparameters and features were obtained, models were built using the training and validation sets, and performance was evaluated in the testing set. Models were created using the primary dataset only and by combining the primary and external datasets.

All statistical analyses were performed in R (v 3.5.0; R Foundation for Statistical Computing, 2018). All prognostic modeling and visualization were performed using an institutional rtemis[23] package for machine learning and visualization in R (https://github.com/egenn/rtemis). The performance of each model was assessed by calculating the balanced accuracy and area under the curve (AUC) on each left-out set. The mean balanced accuracy and AUC across 10 resamples were reported. Comparisons between models were made by testing whether the distributions of calculated AUCs between two models were statistically different using the non-parametric Wilcoxon test.

Heatmaps were created based on pairwise Pearson correlations among features and arranged by hierarchical clustering to explore the relationships between features and studied outcomes. Univariate Cox analyses (UVA) were performed for time to LF and OS, and logistic regression was performed for WHO grade. Variables with $P < .10$ were included in subsequent multivariate analyses (MVA). Recursive partitioning analysis (RPA) was performed using the *rpart* R package with default settings, with the optimal initial number of splits determined by 10-fold cross-validation. The resulting tree was pruned by applying a log-rank *P*-value threshold of less than .10 for each split. Clinical outcomes were estimated using the Kaplan–Meier method and compared using log-rank tests. Contingency tests were performed using Fisher's exact and chi-squared tests.

Results

Patients, Meningiomas, and Outcomes

On the basis of eligibility criteria of available clinical follow-up data, preoperative imaging suitable for quantitative analyses, and available tissue for re-evaluation according to contemporary diagnostic criteria, we identified 303 patients who underwent resection of 314 meningiomas at the University of California San Francisco and the University of Toronto (Tables 1 and 2) from 1990 to 2017. The median age at presentation was 59 years (range: 14–89 years). One hundred ninety-one patients were female (63%) and 112 were male (37%). Seventy meningiomas (22%) were recurrent. There were 179 WHO grade I (57%), 110 WHO grade II (35%) and 25 WHO grade III meningiomas (8%). The median meningioma volume was 30.2 cm^3 (range: 0.40–335.3 cm^3), as calculated from three-dimensional volumetric contours. GTR was achieved in 176 cases (56%), and 59 meningiomas received adjuvant radiation (19%). With a median follow-up of 4.3 years (range: 0–16 years) in the primary dataset (Table 1), the Kaplan–Meier 5-year LFFR estimates were 86%, 58%, and 40%, and the 5-year OS estimates were 89%, 73%, and 49% for WHO grade I, WHO grade II and WHO grade III meningiomas, respectively.

Preoperative MR Imaging Features Are Prognostic for Meningioma Grade, Local Failure and Overall Survival

To identify preoperative MR imaging features with prognostic significance for meningioma grade and/or clinical outcomes, 16 radiologic features were annotated from preoperative imaging studies from the primary dataset (Table 3 and Figure 1A). ADC hypointensity (chi-square test, $P = .0001$, positive-predictive value [PPV] 70%, sensitivity/specificity [S/Sp] 46% and 81%, respectively), peritumoral edema ($P < .0001$, PPV 57%, S/Sp 87% and 39%), absence of a CSF cleft sign ($P < .0001$, PPV 76%, S/Sp 35% and 89%), and indistinct tumor margins ($P = .001$, PPV 90%, S/Sp 18% and 98%) were associated with high grade meningioma (WHO grade II or III). UVA using the primary dataset revealed that radiologic features of tumor diameter ≥5.6 cm (threshold determined by optimal cutoff of the receiver operating characteristics [ROC] curve, $P = .0003$), midline tumor location ($P = .02$), multifocality

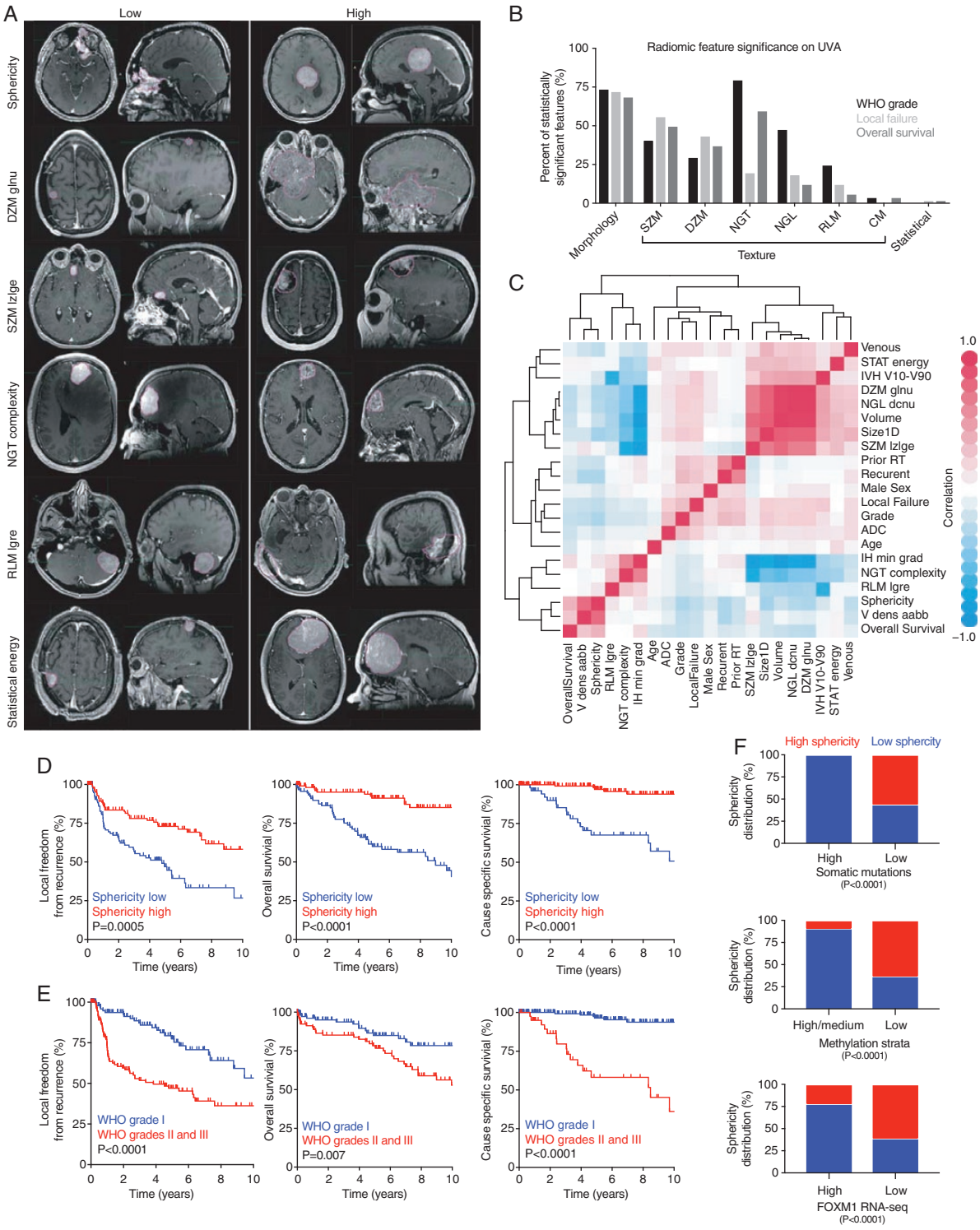

Fig. 2 Radiomic features with prognostic significance for meningioma. (**A**) Radiomic feature examples illustrating low and high values, including morphologic sphericity, distance zone matrix—gray-level non-uniformity (DZM glnu), size zone matrix—large zone low gray-level emphasis (SZM lzlge), neighborhood gray tone—complexity (NGT complexity), run length matrix—low gray-level run emphasis (RLM lgre) and statistical energy. (**B**) Relative radiomic feature category importance for prognostication of meningioma grade, LF or OS based on UVA. The percentage of significant features from each category is shown on the y-axis. The morphology category (29 features) contained the greatest proportion of prognostic features. Textural features showed heterogeneous prognostic value; among these, NGT had a high proportion of significant features for grade and OS that was likely confounded by the small number of features ($N = 5$). (**C**) Pairwise Pearson correlation heatmaps of selected radiomic

($P = .0001$), peritumoral edema ($P = .015$), venous sinus involvement ($P = .002$), absence of a CSF cleft sign ($P = .010$), ADC hypointensity ($P < .0001$) and indistinct margins ($P = .01$) were associated with LF (Supplementary Table 1). Furthermore, MVA using the primary dataset confirmed the prognostic significance of meningioma location (HR 1.27, 95% CI 1.02–1.56, $P = .03$), multifocality (HR 2.57, 95% CI 1.53–4.30, $P = .001$), venous sinus involvement (HR 1.79, 95% CI 1.02–3.13, $P = .04$) and ADC hypointensity (HR 1.87, 95% CI 1.14–3.09, $P = .01$) for LF (Supplementary Table 1). Finally, MVA using the combined primary and external datasets demonstrated that multifocality (HR 2.13, 95% CI 1.29–3.54, $P = .003$) and ADC hypointensity (HR 1.96, 95% CI 1.22–3.14, $P = .005$) were independently associated with meningioma LF (Supplementary Table 1).

To identify radiologic features associated with OS from meningioma, UVA was performed and identified that meningioma diameter ≥5.6 cm ($P = .009$), peritumoral edema ($P = .003$), contrast enhancement ($P = .035$), absence of a CSF cleft sign ($P = .006$), ADC hypointensity ($P = .0003$) and indistinct margins ($P = .0008$) to be associated with worse OS in the primary dataset (Supplementary Table 2). Consistently, MVA using the primary dataset revealed that contrast enhancement (HR 2.42, 95% CI 1.14–5.13, $P = .02$) and ADC hypointensity (HR 3.30, 95% CI 1.68–6.49, $P = .0005$) were independently associated with worse OS. MVA analysis using the combined dataset confirmed that ADC hypointensity (HR 2.36, 95% CI 1.27–4.36, $P = .006$) was independently prognostic for worse patient survival (Supplementary Table 2).

Given the abundance of preoperative radiologic features independently associated with adverse meningioma outcomes, we performed RPA using the primary dataset to identify radiologic risk strata. We identified four distinct LF risk strata based on meningioma multifocality, tumor diameter, and ADC intensity. Multifocal tumors were associated with the lowest LFFR, and smaller, unifocal tumors with diameter <5.6 cm and high ADC were associated with comparatively greater LFFR (Figure 1B and C). Consistently, there was an enrichment of high grade meningiomas in high-risk LFFR strata (Figure 1D). RPA of preoperative radiologic features with respect to OS similarly revealed four risk strata based on ADC intensity, peritumoral edema, and bone involvement (Figure 1E and F), with an enrichment of high grade meningiomas in high-risk OS strata (Figure 1F). After stratification by grade, ADC intensity remained discriminative for LFFR among WHO grade II meningiomas ($P = .013$, log-rank test), and demonstrated a trend toward significance for OS in WHO grade II and grade III meningiomas ($P = .055$ and $P = .074$, respectively, log-rank test). Moreover, the radiologic risk strata we report retained prognostic significance for LFFR and OS when excluding recurrent tumors and restricting analysis to primary meningiomas (Supplementary Figure 2A), and in the external dataset, ADC accurately discriminated between low and higher grade meningiomas ($P = .036$, Fisher's exact test)

Evolving understanding of meningioma biology has identified somatic mutation burden,[18,24] DNA methylation status,[18,25,26] and expression of the pro-mitotic transcription factor *FOXM1*[18,27] as negative prognostic factors for meningioma outcomes. To determine if radiologic risk strata for meningioma LF or OS corresponded to molecular markers of aggressive meningioma, we analyzed the distribution of radiologic strata in the context of molecular features from cases where both sets of information were available from prior whole exome sequencing, 850 k DNA methylation profiling, and RNA sequencing.[18] Consistent with the known role of high somatic mutation burden, high DNA methylation, and high *FOXM1* expression in aggressive meningioma, we found that meningiomas from high-risk radiologic strata were enriched in each of these adverse molecular features (Figure 1H–J). In sum, these data indicate that preoperative MR imaging radiologic features can be used to accurately identify biologically aggressive meningiomas.

Preoperative MR Imaging Radiomic Features Are Prognostic for Meningioma Grade, Local Failure, and Overall Survival

To investigate the prognostic utility of quantitative radiomic features for meningioma grade and clinical outcomes, a comprehensive set of radiomic features was extracted from tumor contoured on preoperative three-dimensional T1 post-contrast MR images (Table 3 and Figure 2A). Radiomic data were categorized into (1) morphologic features, which capture information related to tumor size and shape; (2) textural features, which capture information related to the voxel-by-voxel variation and spatial arrangement of gray-level intensities; and (3) statistical features, which capture statistical measures of the distribution of voxel intensities. UVA was performed on each radiomic feature in relation to meningioma grade, LF, and

Fig. 2 *Continued*
features to tumor volume, ADC, grade, LF, and OS. Rows and columns have been arranged by hierarchical clustering to reveal each feature's relationship to the outcomes of interest. Red denotes positive correlations and blue denotes negative correlations. (**D**, **E**) Kaplan–Meier curves for LFFR, OS and cause specific survival stratified according to meningioma sphericity or WHO grade. (**F**) Low sphericity meningiomas exhibit high somatic mutation burden as identified by whole exome sequencing, high DNA methylation, and high *FOXM1* expression as identified by RNA sequencing, consistent with aggressive tumor biology.[18] The number of somatic mutations was dichotomized at the mean to assign mutation burden, methylation clusters were generated by unsupervised hierarchical clustering of the top 2000 most variable probes, and *FOXM1* expression from RNA-seq was dichotomized at the median. ADC, apparent diffusion coefficient; CM, co-occurrence matrix; dcnu, dependence count non-uniformity; DZM, distance-zone matrix; glnu, gray-level non-uniformity; IH min grad, intensity histogram—minimum gradient; IVH, intensity volume histogram; LF, local failure; LFFR, local freedom from recurrence; lgre, low gray-level run emphasis; lzlge, large zone low gray-level emphasis; OS, overall survival; NGL, neighborhood gray level; NGT, neighborhood gray tone; RLM, run length matrix; RNA-seq, RNA sequencing; RT, radiotherapy; STAT, statistical; SZM, size-zone matrix; UVA, univariate analysis; V dens aabb, volume density—axis-aligned bounding box; WHO, World Health Organization. Analyses are based on the primary dataset.

A

Clinical Models	Grade		Local Failure		Overall Survival	
	Accuracy	AUC	Accuracy	AUC	Accuracy	AUC
Demographic	0.67	0.71	0.67	0.70	0.66	0.71
Therapy	0.70	0.73	0.68	0.69	0.64	0.67
Grade	NA	NA	0.70	0.71	0.68	0.69
Imaging Models						
Radiologic	0.62	0.68	0.60	0.62	0.63	0.65
Radiomic	0.65	0.71	0.61	0.68	0.67	0.75
Combined Models						
Radiologic + Radiomic	0.65	0.71	0.63	0.69	0.67	0.74
Demographic + Therapy + Grade	NA	NA	0.68	0.77	0.64	0.71
Demographic + Radiologic + Radiomic	0.71	0.78	0.67	0.73	0.70	0.77
Demographic + Radiologic + Radiomic + Therapy + Grade	NA	NA	0.67	0.75	0.69	0.77

B

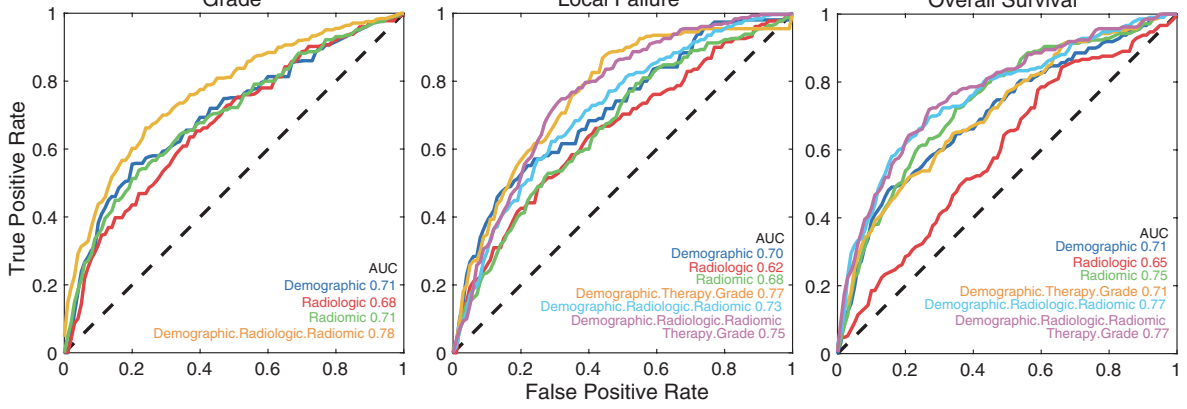

C

Grade

Variable	HR (95% CI)	P-value
Male sex		0.739
Recurrent		0.703
Prior RT		0.991
Multifocal	4.95 (1.76–15.50)	0.004
GTR		0.108
Size 1D		0.433
ADC low	5.56 (2.01–16.70)	0.002
Edema	3.55 (1.40–9.59)	0.009
CSF Cleft	0.26 (0.08–0.80)	0.021
Indistinct margin		0.985
Venous involvement		0.451
Sphericity low		0.560
SZM zone size entropy		0.692
DZM zone distance uniform.		0.970

Local Failure

Variable	HR (95% CI)	P-value
Male sex		0.230
Recurrent	2.4 (1.2–5.1)	0.010
Prior RT		0.175
Multifocal		0.176
GTR	0.6 (0.3–1.0)	0.020
WHO grade II/III		0.155
Diameter	1.9 (1.0–3.5)	0.050
ADC low		0.520
Edema		0.604
Indistinct margin		0.795
Venous involvement		0.223
Sphericity low	2.0 (1.1–3.5)	0.020
SZM zone size entropy		0.336
DZM zone distance uniform.		0.737

Overall Survival

Variable	HR (95% CI)	P-value
Age	1.05 (1.02–1.09)	0.001
Recurrent		0.530
Prior RT		0.040
GTR	0.49 (0.25–0.96)	0.040
Adj RT		0.740
WHO grade II/III		0.160
Diameter		0.201
ADC low		0.080
Edema		0.990
Indistinct margin		0.353
Sphericity low	2.94 (1.47–5.56)	0.002
SZM zone size entropy		0.634
DZM zone distance uniform.		0.725

Fig. 3 Unified prognostic models for meningioma outcomes. (**A**) Performance summary table of prognostic models (clinical, imaging, and combined) showing mean balanced accuracy and AUC of the receiver-operator characteristic curves for prediction of meningioma grade, LF, or OS. (**B**) Receiver-operator characteristic curves of selected prognostic models for grade, LF, and OS demonstrate that the inclusion of preoperative radiologic and radiomic features enhance the accuracy of outcomes predictions. (**C**) Multivariate analyses incorporating clinical, radiologic and radiomic variables to predict meningioma grade, LF, and OS. All analyses are based on the combined primary and external datasets. ADC, apparent diffusion coefficient; AUC, area under the curve; DZM, distance-zone matrix; GTR, gross total resection; LS, local failure; OS, overall survival; RT, radiotherapy; SZM, size-zone matrix; WHO, World Health Organization.

OS. The morphologic category contained the largest proportion of significant radiomic features, with greater than 70% reaching statistical significance on UVA for grade, LF, and OS (Figure 2B). There was substantial variation in the proportion of textural radiomic features reaching statistical significance, and fewer than 5% of statistical features were

significantly associated with meningioma grade, LF, or OS (Figure 2A).

Associations between radiomic features from morphologic, textural, and statistical categories to demographic, therapy, grade, outcome, and radiologic variables were examined (Figure 2C). We identified significant correlation between meningioma SZM and DZM radiomic textural features with meningioma volume, indicating that these radiomic features may be confounded by meningioma size. We also discovered significant correlation between OS and the morphological radiomic features of sphericity and volume density, which were only weakly correlated with meningioma volume. Principal component analysis of morphological radiomic features confirmed the existence of a primary component (40.3% of variance) that was only weakly correlated with tumor volume (Pearson R –0.35) and contained sphericity as the variable with the highest loading factor. Thus, sphericity was selected for further investigation based on variable importance within the morphologic feature category, relatively low correlation with tumor volume (Pearson R –0.18), and ease of interpretation.

UVA and MVA in the primary dataset demonstrated that sphericity was significantly associated with LF and OS, and MVA using the combined dataset confirmed that low sphericity was independently associated with LF (HR 2.66, 95% CI 1.64–4.35, $P < .0001$) and worse OS (HR 3.57, 95% CI 1.92–6.76, $P < .0001$) (Supplementary Tables 1 and 2). Indeed, meningioma sphericity provided comparable stratification of LFFR, OS and cause specific survival relative to WHO grade in the primary dataset (Figure 2D, E). After stratification by WHO grade, sphericity remained highly discriminative for LFFR in grade I meningiomas ($P = .0003$, log-rank test) and for OS in grade II and III meningiomas ($P = .0006$ and $P = .008$, respectively, log-rank test). Sphericity also retained prognostic significance for LFFR and OS when excluding recurrent tumors and restricting analysis to primary meningiomas (Supplementary Figure 2). In the external dataset, sphericity accurately discriminated between low and higher grade meningiomas ($P = .025$, ANOVA) (Supplementary Figure 3). Finally, we found that meningiomas with low sphericity had elevated somatic mutations, DNA methylation, and *FOXM1* expression (Figure 2F).[18] Thus, consistent with radiologic analyses, these data suggest that radiomic features derived from preoperative MR imaging can be used to accurately identify biologically aggressive meningiomas.

Integrated Models Incorporating Demographic, MR Imaging, Radiologic and Radiomic, Treatment and Pathologic Features Provide Accurate Estimates of Meningioma Outcome

To investigate whether preoperative radiologic or radiomic features impart additive prognostic value to traditional clinical variables such as patient demographics, meningioma grade, or therapy (eg, extent of resection and adjuvant radiation), we constructed integrated clinical prognostic models using the random forest method (Figure 3, B). In order to reduce bias and overfitting, a supervised feature reduction approach[22] was applied to the large number of radiomic features, and the final variables included in prognostic models are shown in Table 3. Compared to the traditional clinical model of meningioma stratification according demographic, grade and therapeutic data, the addition of radiologic and radiomic features did not appear to add prognostic value for LF (AUC 0.77 vs 0.75, $P = .79$, Wilcoxon test). In contrast, the addition of radiologic and radiomic features added significant value to prognostic models of meningioma grade (AUC 0.71 vs 0.78, $P = .001$, Wilcoxon test) and OS (AUC 0.71 vs 0.77, $P < .0001$, Wilcoxon test) (Figure 3A, B). Moreover, integrated prognostic models consistently improved in performance when the external dataset was combined with random forest models derived from the primary dataset, indicating a gain of training with additional data (Supplementary Figure 4).

Cox analyses were performed using the primary and combined datasets to validate random forest models of meningioma grade, LF, and OS (Figure 3C and Supplementary Tables 3 and 4). Demographic, therapy, grade, and radiologic variables with $P < .10$ on UVA were included in MVA, as were representative radiomic features within the top three radiomic feature categories: sphericity, SZM (size zone entropy) and DZM (zone distance entropy), each of which had the highest loading factor within the first principal component of their respective radiomic category. In general, all statistically significant variables in the primary dataset were also significant in the combined dataset. With respect to the latter, multifocal meningioma (HR 4.96, 95% CI 1.76–15.5, $P = .004$), ADC hypointensity (HR 5.56, 95% CI 2.01–16.7, $P = .002$), peritumoral edema (HR 3.55, 95% CI 1.4–9.59, $P = .009$) and absence of a CSF cleft sign (HR 0.26, 95% CI 0.08–0.80, $P = .021$) were independently prognostic for high meningioma grade. Recurrent presentation (HR 2.49, 95% CI 1.25–4.63, $P = .01$), GTR (HR 0.60, 95% CI 0.29–0.90, $P = .0195$), meningioma diameter (HR 1.86 per cm, 95% CI 1.00–3.47, $P = .05$) and low sphericity (HR 2.0, 95% CI 1.1–3.5, $P = .02$) were independently associated with LF. Finally, age (HR 1.05 per year, 95% CI 1.02–1.09, $P = .001$), GTR (HR 0.49, 95% CI 0.25–0.96, $P = .0195$), and low sphericity (HR 2.94, 95% CI 1.47–5.56, $P = .002$) were independently prognostic for worse OS.

Discussion

Key Findings

We identify that radiologic and radiomic features extracted from preoperative MR imaging are prognostic for meningioma grade, LF, and OS. By combining traditional clinical variables for stratifying meningioma patients with preoperative imaging features, we develop integrated models with significant prognostic value for meningioma outcomes. Among the comprehensive radiologic and radiomic features we investigated, we find that ADC hypointensity and low tumor sphericity are particularly associated with high grade meningioma, poor local control, and worse OS.

Prognostic Radiologic Features for Meningioma

Prior investigations of qualitative MR imaging features in meningioma have identified ADC hypointensity as prognostic for tumor recurrence.[9] Likewise, peritumoral edema,[9,28,29] irregular meningioma shape,[28]

heterogeneous post-contrast enhancement,[28] and the absence of a CSF cleft sign[28,29] are associated with high meningioma grade and/or worse clinical outcomes. Our findings corroborate these data by validating peritumoral edema, ADC hypointensity, lack of a CSF cleft sign, and indistinct tumor margins as prognostic factors for high grade meningiomas. Moreover, we report the PPV, sensitivity and specificity of each of these features, and perform RPA to identify distinct radiologic risk strata for LF and OS. We find that ADC hyperintensity and the absence of peritumoral edema are associated with WHO grade I meningiomas with excellent OS. ADC similarly discriminates LF among WHO grade II tumors, likely owing to the greater spectrum of clinical behavior and ADC intensity in atypical meningioma.[5,30,31] Thus, like MIB1 proliferation index, ADC may represent a useful marker to identify WHO grade II meningiomas that are at greater risk for recurrence, and for which more aggressive adjuvant therapy or close post-treatment imaging surveillance may be warranted.[5]

Prognostic Radiomic Features for Meningioma

Recent studies in head and neck, brain, lung and other cancers have demonstrated the utility of radiomics in providing valuable prognostic information beyond traditional clinical variables.[11,15,16] Indeed, radiomic techniques can be used to predict meningioma grade preoperatively, a finding that we corroborate.[12] Moreover, we demonstrate that comprehensive imaging analysis can shed light on meningioma LF and OS by incorporating both radiomic and radiologic features into integrated prognostic models and adjusting for clinical covariates in multivariate analysis. Perhaps unsurprisingly, we find that many of the most prognostic radiomic features are highly correlated with tumor size, an important confounding variable which itself is closely correlated with meningioma outcomes. A previous study also identified tumor volume to be highly predictive for survival, with a concordance indices (a measure of predictive performance similar to the area-under-the-curve approach to ROC analysis) of 0.68 and 0.63 for tumor volume compared to 0.69 and 0.65 for radiomic variables for head and neck cancer and lung cancer, respectively.[11] Although these differences were statistically significant, it remains to be established whether radiomic features provide additional clinically significant prognostic value after tumor size is considered. We attempted to account for this in our analysis by adjusting for tumor size in multivariate analysis. In addition, we identify tumor sphericity to be a morphologic feature that is weakly correlated with tumor size, but which is significantly associated with OS. Thus, we propose that ADC hypointensity and low sphericity are two preoperative imaging-derived predictors of poor outcomes in patients with meningioma. Clinically, these two imaging parameters may help risk stratify patients both pre- and postoperatively, particularly those with atypical meningioma.

Strengths and Limitations

The strengths of this study in comparison to prior studies include the relatively large multi-institution sample size, the availability of high quality outcomes data for both LF and OS, the use of standardized image processing and radiomic imaging features to reduce heterogeneity across MR imaging studies, and the availability of demographic and clinical data for patients, all of which facilitated robust multivariate analysis with adjustment of covariates for model creation.

Nevertheless, our study has several important limitations. First, both the primary and external dataset meningiomas were imaged on a mixture of 1.5 and 3T MR scanners, which could add variability to feature annotation and calculation. Fortunately, intensity correction was integrated into our processing steps and our analysis isolated ADC hypointensity and sphericity, which have low dependence on magnet strength. Second, the generalizability of our data is limited insofar as our independent external dataset that did not represent grade II and III meningiomas in the same proportion has our primary dataset. However, all of the meningiomas in our study were graded according to current diagnostic criteria.[1] Given the long natural history of meningioma and the relatively recent change in meningioma grading,[32] other institutional databases will likely require extensive pathologic re-evaluation before the accuracy of our models can be validated in larger independent cohorts. Third, although we were able to identify associations between molecular, radiologic, and radiomic predictors of adverse meningioma outcomes, the number of cases with available molecular data was too low to include somatic mutation burden, DNA methylation profile, or *FOXM1* expression into our integrated prognostic models. Fourth, our clinical data were collected by retrospective chart review which may be subject to selection bias. The recent emergence of prospective meningioma trials may help to ameliorate this limitation,[7,33] but as of yet, no imaging aims have been proposed or reported from these endeavors. Finally, the meningiomas included in this study were relatively heterogeneous, and included both primary and recurrent tumors, but secondary analyses limited to primary meningiomas corroborated our findings.

Conclusions

When considered alongside demographic information, extent of resection, adjuvant radiotherapy and meningioma grade, preoperative radiologic and radiomic features impart important prognostic information for meningioma outcomes. ADC hypointensity and sphericity are of particular value, and could be used to guide clinical risk stratification by predicting tumor grade, LF, and OS in patients with meningioma.

Supplementary Material

Supplementary material is available at *Neuro-Oncology Advances* online.

Keywords

diffusion weighted imaging | magnetic resonance imaging | meningioma | quantitative imaging | radiomics.

Funding

This work was supported by grants from the Wolfe Meningioma Program Project to S.T.M., N.O-B., J.E.V-M., M.W.M., and D.R.R., the National Institutes of Health (1F32CA213944-01) to S.T.M., and the UCSF Brain Tumor Center SPORE to D.R.R.

Conflict of interest statement. The authors have no conflicts of interest concerning the methods or findings of this paper.

Authorship statement: Data collection and analysis: O.M., W.C.C, F.N., M.S., S.T.M., H.N.V., A.W., M.V., E.D.G., G.V., M.P., P.A-L., A.C., Y.I., S.M., K.T., N.A.O.B., A.P., G.Z., M.W.M., J.E.V-M., and D.R.R.; study design and supervision: O.M., T.D.S., S.E.B., P.K.S., S.E.B., A.P., J.E.V-M., and D.R.R.; critically revised and approved the manuscript: All authors.

References

1. Louis DN, Perry A, Reifenberger G, et al. The 2016 World Health Organization classification of tumors of the central nervous system: a summary. *Acta Neuropathol.* 2016;131(6):803–820.
2. Ostrom QT, Gittleman H, Liao P, et al. CBTRUS Statistical Report: primary brain and other central nervous system tumors diagnosed in the United States in 2010–2014. *Neuro Oncol.* 2017;19(suppl 5):v1–v88.
3. Rogers L, Barani I, Chamberlain M, et al. Meningiomas: knowledge base, treatment outcomes, and uncertainties. A RANO review. *J Neurosurg.* 2015;122(1):4–23.
4. Yamasaki F, Yoshioka H, Hama S, Sugiyama K, Arita K, Kurisu K. Recurrence of meningiomas. *Cancer.* 2000;89(5):1102–1110.
5. Chen WC, Magill ST, Wu A, et al. Histopathological features predictive of local control of atypical meningioma after surgery and adjuvant radiotherapy. *J Neurosurg.* 2018;130(2):443–450.
6. Hammouche S, Clark S, Wong AH, Eldridge P, Farah JO. Long-term survival analysis of atypical meningiomas: survival rates, prognostic factors, operative and radiotherapy treatment. *Acta neurochir (wien).* 2014;156(8):1475–1481.
7. Rogers L, Zhang P, Vogelbaum MA, et al. Intermediate-risk meningioma: initial outcomes from NRG oncology RTOG 0539. *J Neurosurg.* 2018;129(1):35–47.
8. Walcott BP, Nahed BV, Brastianos PK, Loeffler JS. Radiation treatment for WHO grade II and III meningiomas. *Front Oncol.* 2013;3:227.
9. Hwang WL, Marciscano AE, Niemierko A, et al. Imaging and extent of surgical resection predict risk of meningioma recurrence better than WHO histopathological grade. *Neuro oncol.* 2016;18(6):863–872.
10. Ildan F, Erman T, Göçer Al, et al. Predicting the probability of meningioma recurrence in the preoperative and early postoperative period: a multivariate analysis in the midterm follow-up. *Skull base.* 2007;17(3):157–171.
11. Aerts HJ, Velazquez ER, Leijenaar RT, et al. Decoding tumour phenotype by noninvasive imaging using a quantitative radiomics approach. *Nat Commun.* 2014;5:4006.
12. Coroller TP, Bi WL, Huynh E, et al. Radiographic prediction of meningioma grade by semantic and radiomic features. *PLoS One.* 2017;12(11):e0187908.
13. Coroller TP, Grossmann P, Hou Y, et al. CT-based radiomic signature predicts distant metastasis in lung adenocarcinoma. *Radiother Oncol.* 2015;114(3):345–350.
14. Lambin P, Rios-Velazquez E, Leijenaar R, et al. Radiomics: extracting more information from medical images using advanced feature analysis. *Eur J Cancer.* 2012;48(4):441–446.
15. Vallières M, Kay-Rivest E, Perrin LJ, et al. Radiomics strategies for risk assessment of tumour failure in head-and-neck cancer. *Sci Rep.* 2017;7(1):10117.
16. Hara JH, Wu A, Villanueva-Meyer JE, et al. Clinical applications of quantitative 3-dimensional MRI analysis for pediatric embryonal brain tumors. *Int J Radiat Oncol Biol Phys.* 2018;102(4):744–756.
17. Morin O, Vallières M, Jochems A, et al. A deep look into the future of quantitative imaging in oncology: a statement of working principles and proposal for change. *Int J Radiat Oncol Biol Phys.* 2018;102(4):1074–1082.
18. Vasudevan HN, Braunstein SE, Phillips JJ, et al. Comprehensive molecular profiling identifies FOXM1 as a key transcription factor for meningioma proliferation. *Cell rep.* 2018;22(13):3672–3683.
19. McHugh ML. Interrater reliability: the kappa statistic. *Biochem Med (Zagreb).* 2012;22(3):276–282.
20. Zwanenburg A, Leger S, Vallières M, Löck S, (for the Image Biomarker Standardisation Initiative). *Image biomarker standardisation initiative.* https://arxiv.org/abs/1612.07003. 2016.
21. Juntu J, Sijbers J, Van Dyck D, Gielen J. Bias field correction for MRI images. Paper presented at: Computer Recognition Systems 2005, 2005; Berlin, Heidelberg.
22. Chatterjee A, Vallières M, Dohan A, et al. An empirical approach for avoiding false discoveries when applying high-dimensional radiomics to small datasets. *IEEE Transactions on Radiation and Plasma Medical Sciences.* 2019;3(2):201–209.
23. Gennatas E. *Towards Precision Psychiatry: Gray Matter Development and Cognition in Adolescence*, Publicly Accessible Penn Dissertations. 2302. https://repository.upenn.edu/edissertations/2302, University of Pennsylvania; 2017.
24. Bi WL, Greenwald NF, Abedalthagafi M, et al. Genomic landscape of high-grade meningiomas. *npj Genomic Med.* 2017;2(1):15.
25. Olar A, Wani KM, Wilson CD, et al. Global epigenetic profiling identifies methylation subgroups associated with recurrence-free survival in meningioma. *Acta Neuropathol.* 2017;133(3):431–444.
26. Sahm F, Schrimpf D, Stichel D, et al. DNA methylation-based classification and grading system for meningioma: a multicentre, retrospective analysis. *Lancet Oncol.* 2017;18(5):682–694.
27. Harmancı AS, Youngblood MW, Clark VE, et al. Integrated genomic analyses of de novo pathways underlying atypical meningiomas. *Nat Commun.* 2017;8:14433.

28. Liu Y, Chotai S, Chen M, Jin S, Qi ST, Pan J. Preoperative radiologic classification of convexity meningioma to predict the survival and aggressive meningioma behavior. *PLoS One*. 2015;10(3):e0118908.
29. Tomura N, Takahashi S, Sakuma I, et al. Neuroradiological findings of atypical meningiomas. *CMIG Extra*. 2004;28(4):33–39.
30. Nagar VA, Ye JR, Ng WH, et al. Diffusion-weighted MR imaging: diagnosing atypical or malignant meningiomas and detecting tumor dedifferentiation. *AJNR Am J Neuroradiol*. 2008;29(6):1147–1152.
31. Tang Y, Dundamadappa SK, Thangasamy S, et al. Correlation of apparent diffusion coefficient with ki-67 proliferation index in grading meningioma. *AJR Am J Roentgenol*. 2014;202(6):1303–1308.
32. Louis DN, Ohgaki H, Wiestler OD, et al. The 2007 WHO classification of tumours of the central nervous system. *Acta Neuropathol*. 2007;114(2):97–109.
33. Weber DC, Ares C, Villa S, et al. Adjuvant postoperative high-dose radiotherapy for atypical and malignant meningioma: a phase-II parallel non-randomized and observation study (EORTC 22042-26042). *Radiother Oncol*. 2018;128(2):260–265.